nature climate change

LETTERS

PUBLISHED ONLINE: 17 JULY 2017 | DOI: 10.1038/NCLIMATE3347

Climate impacts of oil extraction increase significantly with oilfield age

Mohammad S. Masnadi* and Adam R. Brandt

Record-breaking temperatures[1] have induced governments to implement targets for reducing future greenhouse gas (GHG) emissions[2,3]. Use of oil products contributes ∼35% of global GHG emissions[4], and the oil industry itself consumes 3–4% of global primary energy. Because oil resources are becoming increasingly heterogeneous, requiring different extraction and processing methods, GHG studies should evaluate oil sources using detailed project-specific data[5]. Unfortunately, prior oil-sector GHG analysis has largely neglected the fact that the energy intensity of producing oil can change significantly over the life of a particular oil project. Here we use decades-long time-series data from twenty-five globally significant oil fields (>1 billion barrels ultimate recovery) to model GHG emissions from oil production as a function of time. We find that volumetric oil production declines with depletion, but this depletion is accompanied by significant growth—in some cases over tenfold—in per-MJ GHG emissions. Depletion requires increased energy expenditures in drilling, oil recovery, and oil processing. Using probabilistic simulation, we derive a relationship for estimating GHG increases over time, showing an expected doubling in average emissions over 25 years. These trends have implications for long-term emissions and climate modelling, as well as for climate policy.

To date, most greenhouse gas (GHG) analysis of the oil sector has focused on comparing the impacts of oil-derived transport fuels to other transport fuel options. This is a reasonable focus because the largest source of emissions from oil use is generally the combustion of finished fuels (for example, gasoline burned in an automobile). However, emissions from oil and gas extraction and processing are sometimes significant, particularly for unconventional resources or when energy-intensive enhanced oil recovery (EOR) strategies are used. Also from a national perspective, oil and gas extraction can cause a significant fraction of domestic emissions in fossil fuel exporting countries[6] such as Canada (∼20% of national emissions)[7], Russia (∼20%; ref. 8), and Norway (∼28%; ref. 9).

Most large-scale emissions modelling and accounting efforts treat the oil sector simply, often with representative GHG intensities for upstream, refining, and consumption. Just as problematically, nearly all oil and gas emissions estimates rely on 'snapshot' data of varying quality and vintage, neglecting age-related changes in engineering practice (for example, water/gas/steam injection) and processing requirements (for example, fluid separation). Neglecting temporal trends in oil-sector emissions is problematic for long-term climate and integrated assessment modelling, where emissions trends over decades are of interest.

A few prior studies have examined temporal trends in GHG intensity. First, Brandt[10] studied the impact of oil depletion on the energy efficiency of oil extraction and refining in hundreds of California oilfields. He reported increases in energy intensity of crude oil production with depletion due to increased work of lifting of fluids as oilfields age. Gavenas *et al.*[6] also empirically investigated the CO_2 emissions from Norwegian oil and gas extraction, and reported a significant increase in emissions per unit of oil extracted over time.

Such temporal trends are important because they can affect our decisions about the costs and benefits of oil substitutes. Wallington *et al.*[11] argue that neglecting temporal trends ignores the general temporal increase in emissions from depletable resources such as petroleum, and the general decrease in impacts of alternative fuel technologies, attributable to technological advances. Thus, life-cycle analysis (LCA) studies comparing alternative fuel vehicle systems—such as those underpinning the California Low Carbon Fuel Standard (LCFS) and European Fuel Quality Directive (EU FQD)[12–14]—could unfairly disincentivize oil alternatives by ignoring temporal trends in GHG intensity. Such a dynamic analysis is a step in the direction of a 'consequential' analysis framework for crude oil environmental impacts[11].

This paper makes a first attempt to examine the temporal trends in oilfield emissions intensity using a data-rich engineering-based approach. We examine 25 globally important giant oilfields with >1 billion barrels (Gbbl) of estimated ultimate recovery (EUR). We model emissions from these oil fields over the course of decades, computing GHG intensities as a function of time (see Methods).

The life-cycle GHG emissions of each oil field are estimated over time using the open source Oil Production Greenhouse Gas Emissions Estimator (OPGEE)[15]. OPGEE uses characteristics of oilfields along with engineering computations to estimate the energy required to produce, process and transport crude oil, with the unit of analysis being 1 megajoule (MJ) of crude oil delivered to the refinery entrance. Data for the modelled fields were gathered from a variety of public statistics and scientific/technical papers, with nearly 100 sources utilized (see Supplementary Information).

We first generated a semi-quantitative data quality assessment for the 25 modelled fields plotted in Fig. 1. Figure 1 uses a scale ranging from a score of 1 (low quality, red), to a score of 3 (high quality, blue). The parameters classified as being of primary and secondary importance are derived from prior studies which explored importance of parameters on GHG emissions[16].

A score of 1 is applied when OPGEE defaults are used because field-specific data were mostly or completely unavailable. Common examples include the reservoir productivity index and the associated gas treatment system configuration. A score of 2 indicates that partial data were available, but gaps required extrapolations, approximations, or field-level estimates. For example, flaring rates for recent years are collected from spatial analysis of satellite observations, but satellite flaring observations are not available

Department of Energy Resources Engineering, School of Earth, Energy and Environmental Sciences, Stanford University, California 94305, USA.
*e-mail: masnadi@stanford.edu

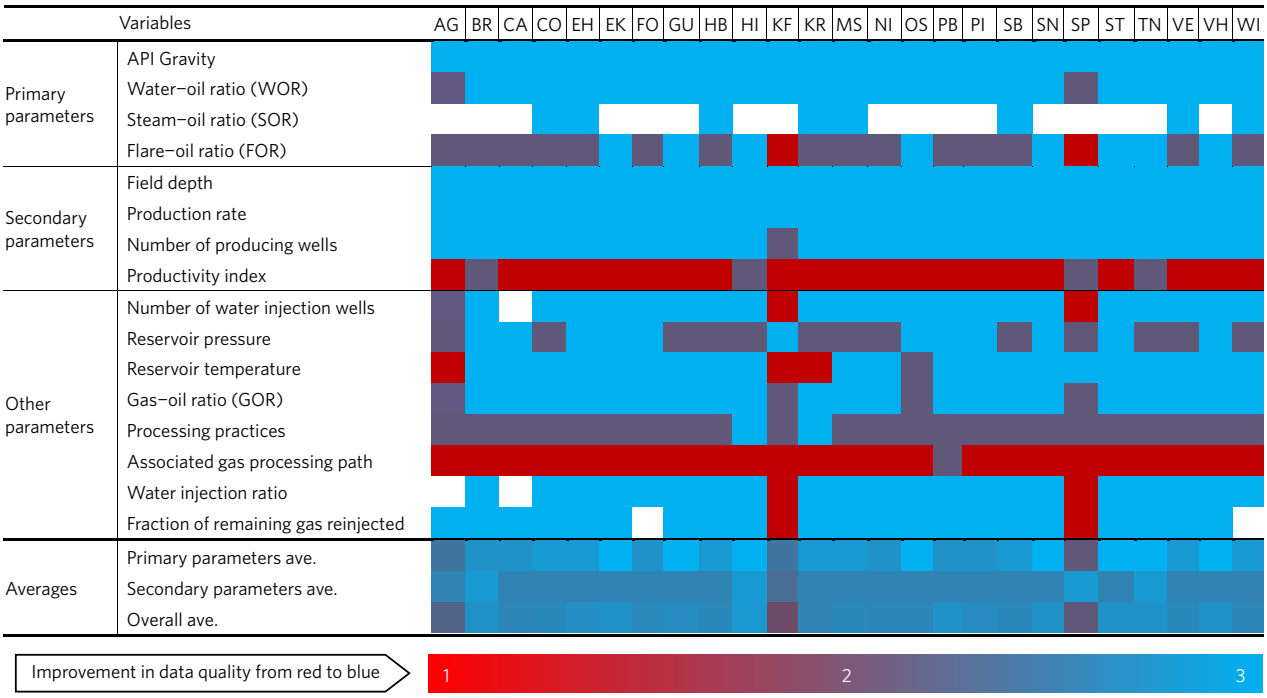

Figure 1 | Oil fields data quality assessment. AG, Agbami; BR, Brent; CA, Cantarell; CO, Coalinga; EH, Elk Hills; EK, Ekofisk; FO, Forties; GU, Gullfaks; HB, Huntington Beach; HI, Hibernia; KF, Kingfish; KR, Kern River; MS, Midway-Sunset; NI, Ninian; OS, Oseberg; PB, Prudhoe Bay; PI, Piper; SB, South Belridge; SN, Snorre; SP, Spraberry Trend; ST, Statfjord; TN, Terra Nova; VE, Ventura; VH, Valhall; WI, Wilmington. White colour squares mean not applicable (N/A—no number) when a parameter is irrelevant for the corresponding field.

over decades. For this reason, in most cases the flare-to-oil ratio (FOR) is given a data quality score of 2. Finally, a score of 3 indicates that high-quality data from government statistics or peer-reviewed literature were available for all (or nearly all) of the modelling period. Note that high-quality data may still subject to some variability or uncertainty associated with mis-measurement or mis-reporting.

Data quality averages (primary, secondary, and overall) shown in Fig. 1 suggest generally satisfactory data quality, with the relative exception of Spraberry Trend (USA) and Kingfish (Australia). These fields are therefore excluded from the probabilistic analysis explained below. Figure 2 shows time-series trends in normalized upstream GHG emissions (g CO_2 eq/MJ crude petroleum) of heavy oil (API gravity $\leq 20°$), medium ($20° <$ API $\leq 30°$), and light (API $> 30°$) crudes. These results cover the period from 1949 to 2015, with years modelled varying by field (see Supplementary Information). The first year plotted for each field is either the first year of production (common) or the earliest year in which data were obtained (uncommon). In Fig. 2, trends are made comparable by normalizing yearly emissions by the earliest observation for that field (for non-normalized results see Supplementary Information datafile). Figure 2 shows that regardless of the crude oil type, per-MJ GHG emissions generally increase over the life of a field. This increase is driven by a decline in natural reservoir pressure and increased energy expenditures on recovery methods such as water injection, steam injection, and gas injection. In addition, increased water production results in more mass lifted and handled per unit of oil produced. The most significant increase in GHG intensities correspond to a Norwegian field, Gullfaks (~13 times), followed by three British fields, Brent (~9 times), Ninian (~8 times), and Piper (~7 times). This is due in part to declines in oil output with depletion, which increases the amount of fluid processed per unit of oil produced.

For example, we can explore the evolution of the Ekofisk field, a major oil and gas field of the North Sea[17]. Ekofisk GHG intensities are low compared to many oilfields due to a highly productive early production process. Emissions intensities declined slowly until 1976 (year 6) due to reservoir-pressure-driven primary production. After 1985, water injection was used to halt pressure declines and improve the extraction rate. Although Ekofisk reached its production peak in 2002 (year 32), GHG intensities continued to increase gradually. By the end of the dataset, Ekofisk oil production declined to ~36% of its peak level whereas the water production rate had increased to over twice that of oil production. More energy is therefore consumed per unit of oil extracted due to increased lifting, handling and processing of fluids[18]. Despite a falling trend in overall production of Norwegian oil and gas fields over the past decade, GHG releases from oil industry activity have not been falling, causing concern in Norway about GHG emissions[6,17,19]. This noted trend is consistent with the patterns observed here.

Reservoir extraction methods also matter. The Kern River field is a good example of this effect. GHG intensities from Kern River first dramatically increased to 39.1 g CO_2 eq/MJ by 1981 (model year 16) due to the introduction of steam injection for enhanced recovery in the 1960s and rapid increases in the rate of injection of steam. During the early 1980s—when the oil price was at a peak because of geopolitical tensions (that is, Iranian revolution and the subsequent Iran–Iraq war) and market imbalances—oil companies took strong measures to boost production. The Kern River field eventually reached a maximum steam–oil ratio (SOR) of 7.6 bbl steam injected per bbl oil produced. After the oil price drop of the late 1980s, such high injection rates were uneconomic and SOR dropped to about 3 bbl steam/bbl oil, where it remained for many years, which reduced emissions significantly. A similar trend occurred in the South Belridge heavy oil field.

In contrast to the general trend of increasing emissions over time, intervention via government regulation can reduce emissions intensity. Two Canadian offshore fields, Hibernia and Tera Nova, provide an example of this effect (see Fig. 3). Emissions intensity from these fields dropped due to regulation-enforced[20] declines

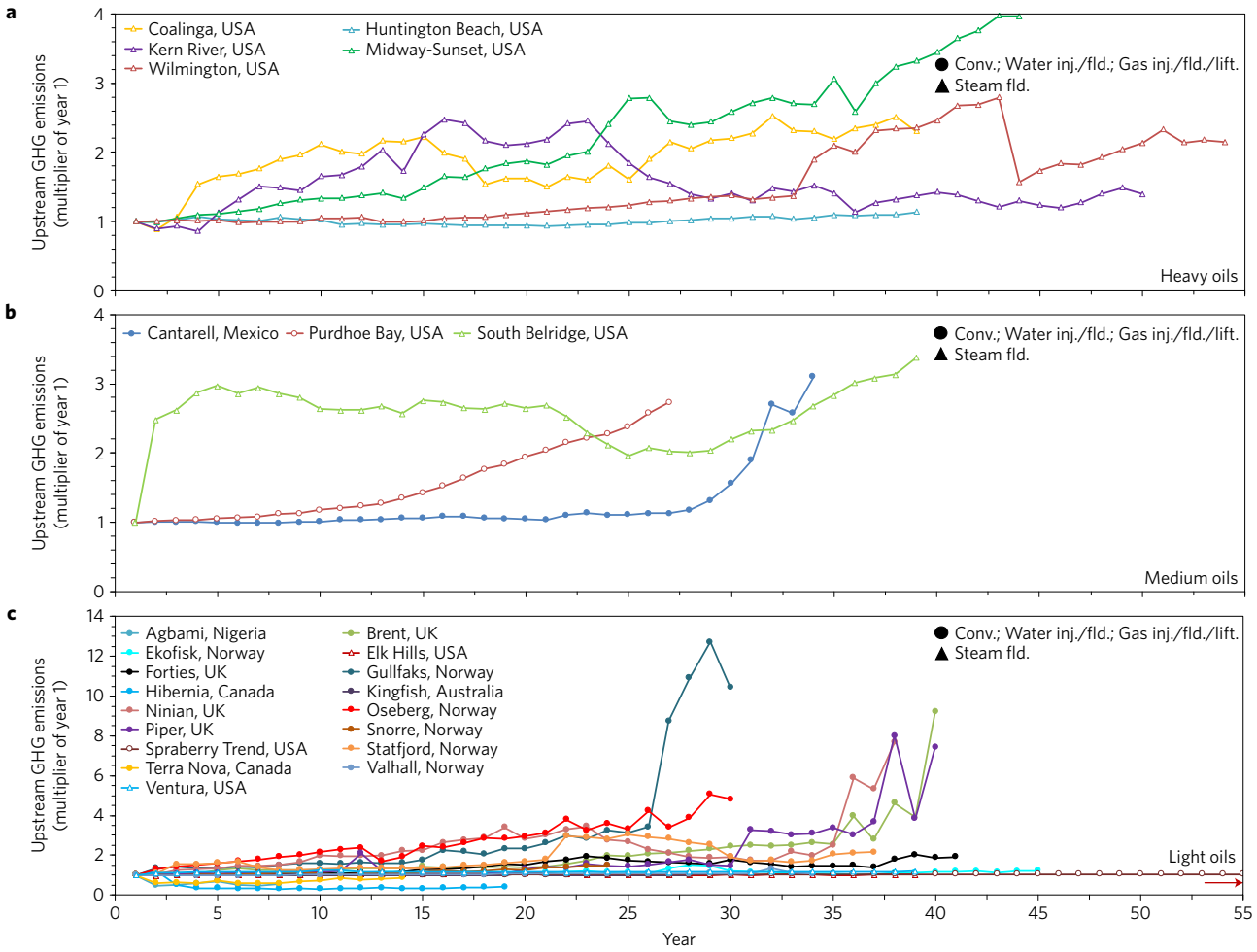

Figure 2 | Time-series trends in normalized upstream GHG intensities of twenty-five global oil fields (offshore and onshore) with different extraction practices (water injection/flooding, gas injection/flooding/lifting, or steam flooding) over the course of production in the period of 1949–2015. a, Heavy oils. **b**, Medium oils. **c**, Light oils. Filled and hollow markers represent offshore and onshore fields, respectively. The Spraberry Trend field GHG intensities follow a similar flat trend as the mid-50s and ends at year 67. See Supplementary Information datafile for underlying data and digital figure.

in flaring of associated gas. Regulation requires oil production rate limitations when flare management systems (for example, gas compression) are out of service[20], resulting in large efforts by operators to curtail flared gas. If the OPGEE default flaring–oil ratio (FOR) for Canada is applied, the usual trends of increasing emissions intensity are observed, but if reported flaring data are used rather than defaults, emissions intensities decline significantly. This highlights the importance of access to actual field data, especially for primary-importance parameters such as FOR.

To derive general trends from the dataset, we perform time-series Monte Carlo analysis of emissions intensity as a function of field age (see Methods), as shown in Fig. 4. In Fig. 4a, we take observations of normalized GHG intensities plotted in Fig. 2 and fit each year with a lognormal distribution (see Methods), then draw 1,000 realizations from each lognormal fit. Each of these draws can be interpreted as a probabilistic sample of one barrel from our sampled fields. Note that although the 25 modelled fields are very different in geologic specifications, oil quality, extraction practices, and so on, the results show overall growth in life-cycle GHG intensities for the majority of realizations, with increasing dispersion in later years, as shown by diverging high and low percentiles. The energetic productivity dynamics of the same fields studied elsewhere[21] are consistent with the presented GHG intensities trends. Figure 4a also plots the oil-volume-weighted mean yearly GHG multiplier, which is generally consistent with the 25 percentile trend. Over the course of 25 years production, the average GHG emissions intensity increases about twofold, while the 95 percentile barrel increases by a factor of ~3.5.

In Fig. 4b we examine the effect of time on the emissions intensity of volume-weighted 'baskets' of crude oil. We create 1,000 realizations of a volume-weighted probabilistic basket where the basket is filled from each sample field in proportion to its production volume. We then compute and plot the time trends in mean emissions of each basket. This is analogous to creating many realizations of the oil-volume-weighted curve in Fig. 4a (dot-dash). Note that dispersion across volume-weighted probabilistic baskets is much less than dispersion for individual crudes, but the upward trend in basket emissions is consistent.

Lastly, Fig. 5 shows modelling parameters derived from Fig. 2. As above, each year's set of normalized multipliers from Fig. 2 is fitted with a lognormal distribution (see Supplementary Information). Figure 5 shows time trends in the normalized GHG intensities mean (μ_t) and standard deviation (σ_t) of the best-fitting lognormal distribution, along with their 95% confidence intervals. Figure 5 shows increases in both the mean and spread of the best-fitting lognormal distribution. Clearly, over time the expected emissions increase (that is, μ_t increases) while the dispersion of results also increases (that is, σ_t increases). In Fig. 5 we perform linear fits to μ_t and σ_t. These equations can be used to model expected emissions multipliers as a function of time, which could be useful for estimating dynamic oil-sector upstream GHG intensities.

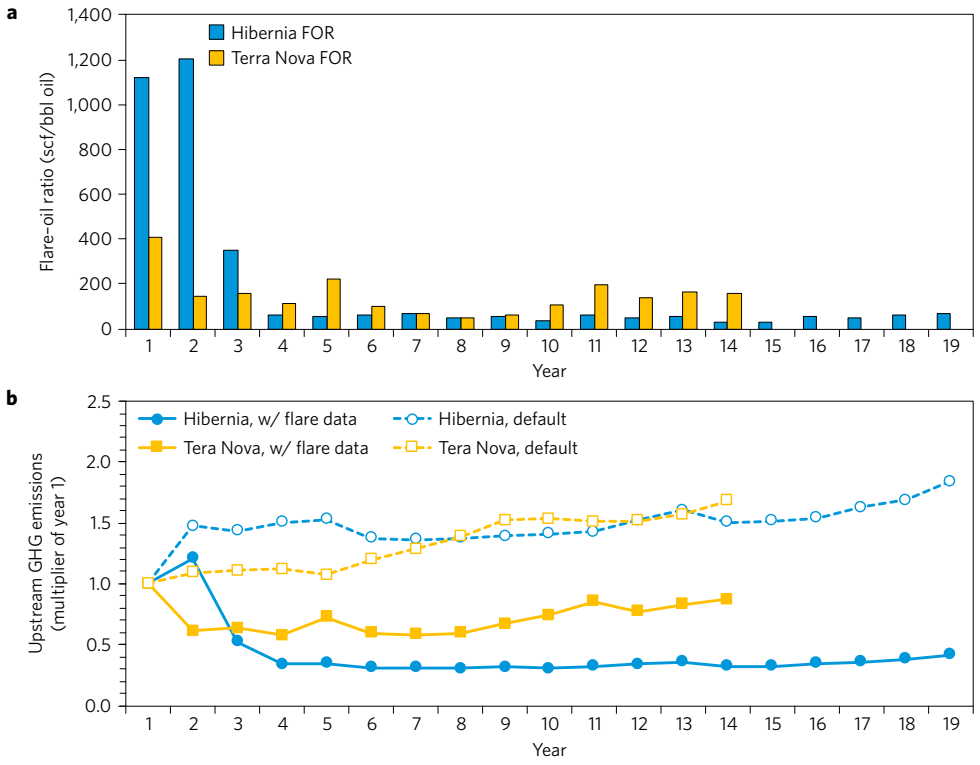

Figure 3 | Effect of FOR on total LCA GHG intensities of two Canadian offshore oil fields (Hibernia and Terra Nova) over the course of production till 2015. a, Hibernia and Terra Nova FOR ratio. **b**, Upstream GHG intensities, default and with flare data.

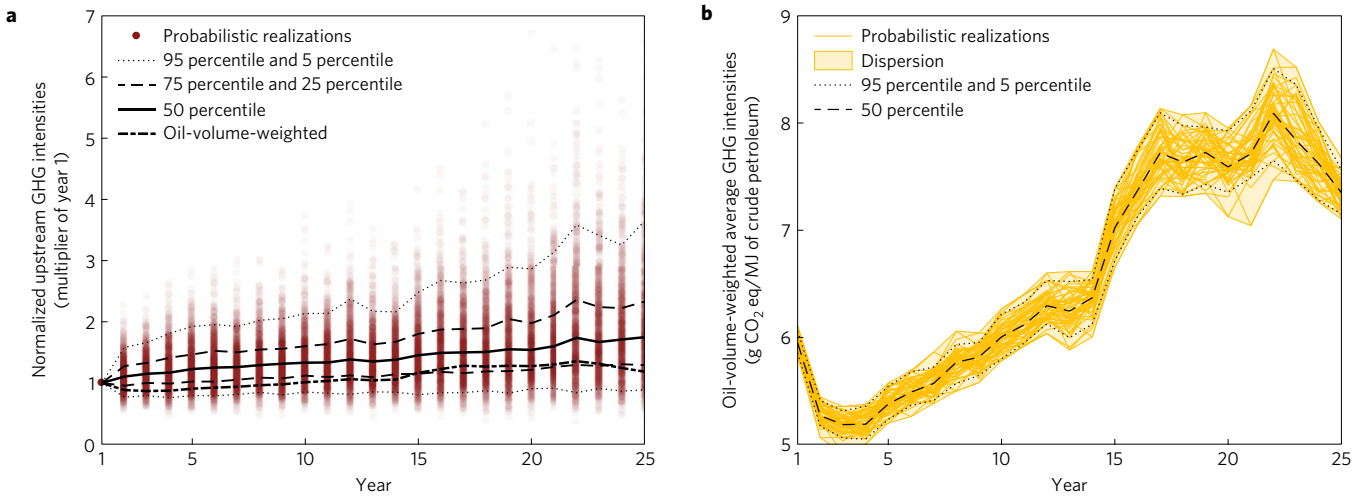

Figure 4 | Probabilistic Monte Carlo GHG intensities dynamics of twenty global giant oilfields. a, Time-series normalized upstream GHG intensities (1,000 realizations per year), statistical percentiles, and oil-volume-weighted mean GHG intensities over the course of 25 years oil production. **b**, Dispersion in oil-volume-weighted average GHG intensities (50 probabilistic realizations from a 'basket' of crudes).

In summary, the per-MJ GHG emissions from oil fields vary from 'oil-to-oil', but also differ significantly 'time-to-time' over a field's productive life. Although in any given oil field carbon intensity (CI) can be estimated given current data, its average CI over its production life is likely to be higher than a snapshot analysis performed at early periods of high productivity. This trend, coupled with the shift to unconventional resources noted elsewhere[11], leads to the important conclusion that the GHG intensities of both average and marginal petroleum resources will probably increase over time. Therefore, long-term analysis should account for these factors so that investors, policymakers, industry, and other stakeholders can adequate compare crudes and assess their climate consequences both before development decisions are made. For example, oil GHG emissions dynamics should be considered for design and allocation of future regulatory smart tax regimes[22]. Such analysis would also assist stakeholders to compare accurately the fossil-based fuels with alternatives and to shape how they address the climate impacts of oil.

Future oil and gas reservoir management should be directed towards both economic and environmental optimization. A clear success story is shown above with Canadian offshore fields flare management[20]. Another example is CO_2 enhanced oil recovery (EOR). CO_2 EOR can simultaneously sequester CO_2 and improve oil recovery[23]. In regions with carbon taxes, this effect is already seen: the Norwegian ministry of climate and environment[24] argues

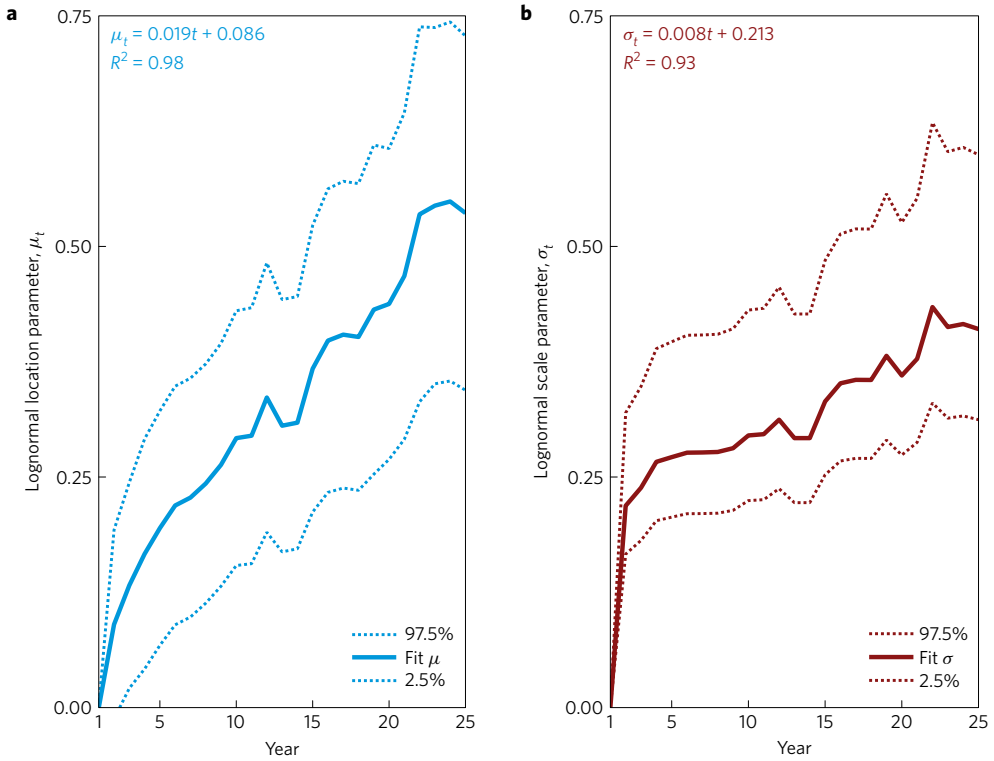

Figure 5 | Time-series normalized GHG intensities mean (μ_t) and standard deviation (σ_t) of lognormal distribution fitting data with fitted first-order polynomial trends.

that their CO_2 tax is likely to have caused the separation and underground storage of the CO_2 content in the gas extracted at the Sleipner field since 1996, and at the Snøhvit field since 2008[6].

Making good decisions in the face of these observed long-term trends requires more information about oil resources. Such transparency is most likely to occur in response to reporting guidelines and regulations that require consistent, comparable, and verifiable data. Improving these analyses is a critical need for development of policies that account for leakage of GHG emissions across regulatory boundaries and to ensure that upstream climate impacts from oil are sufficiently factored into policymaking and decisions about use of petroleum products.

Methods

Methods, including statements of data availability and any associated accession codes and references, are available in the online version of this paper.

Received 26 October 2016; accepted 15 June 2017; published online 17 July 2017

References

1. NASA, NOAA analyses reveal record-shattering global warm temperatures in 2015. *The National Aeronautics and Space Administration* (accessed February 2017); http://www.nasa.gov/press-release/nasa-noaa-analyses-reveal-record-shattering-global-warm-temperatures-in-2015
2. *Paris Agreement* (UNFCCC, 2015).
3. Green Transformation 'Unstoppable' as Countries Agree to Curb Powerful Greenhouse Gases. *United Nations News Centre* (15 October 2016); http://www.un.org/apps/news/story.asp?NewsID=55310#.WAZ4A2WFhuY
4. *Key World Energy Statistics* (Intl. Energy Agency, 2015).
5. Gordon, D., Brandt, A., Bergerson, J. & Koomey, J. *Know Your Oil: Creating a Global Oil-Cimate Index* (Carnegie Endowment for International Peace, 2015); http://carnegieendowment.org/2015/03/11/know-your-oil-creating-global-oil-climate-index-pub-59285
6. Gavenas, E., Rosendahl, K. E. & Skjerpen, T. CO_2 emissions from Norwegian oil and gas extraction. *Energy* **90,** 1956–1966 (2015).
7. *National Inventory Report 1990–2015: Greenhouse Gas Sources and Sinks in Canada: Executive Summary* (Environment Canada, accessed July 2017); https://www.ec.gc.ca/ges-ghg/default.asp?lang=En&n=662F9C56-1
8. *Pathways to an Energy and Carbon Efficient Russia* (McKinsey Company, accessed February 2017); http://www.mckinsey.com/business-functions/sustainability-and-resource-productivity/our-insights/pathways-to-an-energy-and-carbon-efficient-russia
9. *Emissions of Greenhouse Gases* (Statistics Norway, accessed February 2017); http://ssb.no/en/natur-og-miljo/statistikker/klimagassn
10. Brandt, A. R. Oil depletion and the energy efficiency of oil production: the case of California. *Sustainability* **3,** 1833–1854 (2011).
11. Wallington, T. J. *et al*. When comparing alternative fuel-vehicle systems, life cycle assessment studies should consider trends in oil production. *J. Ind. Ecology* **21,** 244–248 (2017).
12. Farrell, A. & Sperling, D. *A Low-Carbon Fuel Standard for California. Part 1: Technical Analysis* (Inst. of Transportation Studies, Univ. of California, 2007).
13. Farrell, A. & Sperling, D. *A Low-Carbon Fuel Standard for California. Part 2: Policy Analysis* (Inst. of Transportation Studies, Univ. of California, 2007).
14. Directive 2009/30/EC of the European Parliament and of the Council of 23 April 2009. *Official J. Eur. Union* **140,** 88–113 (2009).
15. El-Houjeiri, H. M. *et al*. *Oil Production Greenhouse Gas Emissions Estimator (OPGEE) v.2.0a: User Guide Technical Documentation* (2017).
16. Brandt, A. R., Sun, Y. & Vafi, K. Uncertainty in regional-average petroleum GHG intensities: countering information gaps with targeted data gathering. *Env. Sc. Tech.* **49,** 679–686 (2014).
17. Norway Passes the Climate Buck Again. *NEWSinENGLISH* (5 February 2015); http://www.newsinenglish.no/2015/02/05/norway-passes-the-buck-again
18. Devold, H. *Oil and Gas Production Handbook. An Introduction to Oil and Gas Production, Transport, Refining and Petrochemical Industry* (lulu.com, ABB Oil and Gas, 2013); https://library.e.abb.com/public/34d5b70e18f7d6c8c1257be500438ac3/Oil%20and%20gas%20production%20handbook%20ed3x0_web.pdf
19. Norway and the environment. Binge and purge *The Economist* (22 January 2009); http://www.economist.com/node/12970769
20. *Newfoundland and Labrador Offshore Area Gas Flaring Reduction Implementation Plan* (The Canada-Newfoundland and Labrador Offshore Petroleum Board, accessed Februay 2017); http://www.cnlopb.ca/legislation/guidelines.php

21. Masnadi, M. S. & Brandt, A. R. Energetic productivity dynamics of global super-giant oilfields. *Energy Env. Sci.* **10,** 1493–1504.
22. Gordon, D. & Mathews, J. T. *Smart Tax: Pricing Oil for a Safe Climate* (Carnegie Endowment Intl. Peace, 2016); http://carnegieendowment.org/2016/06/15/smart-tax-pricing-oil-for-safe-climate-pub-63765
23. *Resources to Reserves* (Intl. Energy Agency, 2013).
24. *Facts 2014* (Norwegian Petroleum Directorate and Norwegian Ministry of Petroleum and Energy, 2014); http://www.npd.no/en/Publications/Facts/Facts-2014

Acknowledgements

V. Tripathi provided historic data for five oilfields. The Natural Sciences and Engineering Research Council of Canada (NSERC) and Ford Motor Company provided financial support to M.S.M.

Author contributions

Both M.S.M. and A.R.B. were involved in data gathering, processing and analysis of different fields. The final results were integrated and produced by M.S.M. He also wrote the manuscript, and all authors contributed to revising the paper.

Additional information

Supplementary information is available in the online version of the paper. Reprints and permissions information is available online at www.nature.com/reprints. Publisher's note: Springer Nature remains neutral with regard to jurisdictional claims in published maps and institutional affiliations. Correspondence and requests for materials should be addressed to M.S.M.

Competing financial interests

The authors declare no competing financial interests.

Methods

Data processing. Twenty-five large petroleum fields were chosen for this analysis. The selected fields contain at least 1 billion barrels of EUR. Such giant fields are not large in number but account for a large share of global petroleum production[25]. In the USA, we analyse Prudhoe Bay (Alaska), Wilmington, Midway-Sunset, Kern River, Coalinga, Huntington Beach, Ventura, Elk Hills, South Belridge (California), and the Spraberry Trend (Texas). Canadian fields include Hibernia and Terra Nova. We include the Cantarell field in Mexico. In the North Sea we include Brent, Forties, Piper and Ninian from the UK, as well as Ekofisk, Statfjord, Oseberg, Gullfaks, Snorre and Valhall from Norway. Agbami in Nigeria and Kingfish in Australia are also included. A lack of publicly accessible data prevents analysis in numerous major oil-producing regions, including Russia and Saudi Arabia.

The fields selected represent a range of reservoir parameters and production practices. Both onshore and offshore fields are included. Post-primary production practices include water flooding, steam injection, natural gas injection, and nitrogen injection[26]. With regard to known parameters that can have significant impacts on GHG intensity (previously noted 'primary' and 'secondary' parameters of interest[16]), these fields vary in API gravity, water–oil ratio (WOR), flaring rate, field depth, oil production rate, number of wells, and so on.

The life-cycle GHG emissions of each oil field are estimated over time using the open source Oil Production Greenhouse Gas Emissions Estimator (OPGEE) version 2.0a, developed at Stanford University[15]. OPGEE is an engineering-based LCA tool which evaluates upstream oil emissions, including all activities from primary extraction to delivery of crude at the refinery inlet gate. It includes emissions from exploration, drilling and development, production and extraction, surface processing, maintenance, waste disposal, and crude transport[27,28]. The functional unit (or unit of analysis) is 1 MJ of crude petroleum delivered to the refinery entrance gate. OPGEE estimates emissions using engineering models of production processes (for example, water flooding), reservoir characteristics (for example, depth), and processing requirements (for example, application of acid gas removal). When input data are not available, OPGEE supplies defaults based on petroleum engineering literature.

Multiple types of reservoir stimulation and artificial lift are applied to the fields in this analysis. The OPGEE model does not allow for simultaneous modelling of all types of production practices. For example, gas lifting and application of a downhole pump are mutually exclusive scenarios in OPGEE. In such cases the overall field GHG emissions are estimated as the weighted average of each production scenario, with weighting performed according to number of wells applying a given technology. See work by Tripathi[26] for more details. The estimated GHG intensities and oil production data are provided in the 'GHG Intensities & Production Data' Excel file.

Statistical analysis. Before fitting lognormal distributions to each year's results, statistical analysis was performed on normalized GHG intensities from Fig. 2. The Lilliefors test was used to test the fit of each year's observations to five distributions: normal, lognormal, exponential, Weibull, and extreme value (using MATLAB software). Over 25 modelled years, the datasets were found to reject the null hypothesis that the data come from these distributions in 18, 13, 25, 16 and 22 years respectively. The lognormal distribution fit is most satisfactory, being rejected in 13 out of 25 years, including the first 11 model years (no other distribution type performed better in these early years). Due to the fact that the lognormal distribution was favoured by the Lilliefors test, particularly in later observed years, we proceed with a lognormal model. In a one-sample Kolmogorov–Smirnov (KS) test against fitted lognormal distributions, the null hypothesis (that the data are lognormally distributed) is rejected in only 1 out of 25 years (in year 1).

The lognormal distribution is thus fitted to each year's observations, using maximum likelihood methods (MATLAB software), resulting in lognormal μ_t, σ_t, and the 95% confidence interval for each parameter in each model year. These fits are used to generate Monte Carlo realizations in Fig. 4a, as well as the results and equations in Fig. 5.

Monte Carlo simulation. For the probabilistic simulation, we only include fields with an acceptably long time-series, set to field greater than or equal to 25 years of data (this removes Agbami, Hibernia and Terra Nova). We also remove two fields with unacceptable data quality (Spraberry Trend and Kingfish based on Fig. 1). The remaining twenty fields are: Brent, Cantarell, Coalinga, Elk Hills, Ekofisk, Forties, Gullfaks, Huntington Beach, Kern River, Midway-Sunset, Ninian, Oseberg, Prudhoe Bay, Piper, South Belridge, Snorre, Statfjord, Ventura, Valhall, Wilmington.

The Monte Carlo simulation shown in Fig. 4a was performed with 1,000 realizations per year. Estimated μ_t, σ_t from lognormal fits for each year are used to generate normally distributed random variables, which are then scaled exponentially to generate the appropriate lognormally distributed samples. If the corresponding non-transformed means (m_t) and standard deviations (s_t) are desired, they can be computed from μ_t, σ_t using these relationships:

$$\mu_t = \ln\left(\frac{m_t^2}{\sqrt{s_t^2 + m_t^2}}\right) \quad (1)$$

$$\sigma_t = \sqrt{\ln\left(\frac{s_t^2 + m_t^2}{m_t^2}\right)} \quad (2)$$

where μ_t and σ_t are time-series (t) values of fitted lognormal parameters.

To compute the oil-volume-weighted GHG intensity presented in Fig. 4b, baskets of size 1,000 barrels are drawn from the 20 reference fields proportionately to their yearly volumetric oil production share of the basket. Numbers are randomly generated (uniform distribution over [0–1]) and apportioned to one of 20 crudes depending on drawn number and proportional share of each crude (see Supplementary Information worksheet). Next, the corresponding average GHG intensity of each basket of 1,000 samples per year is computed 50 times for all 25 years of production. Therefore, Fig. 4b can be seen as representing the dispersion in an oil-volume-weighted average GHG intensity.

Data availability. To model our sample of oilfields, historical data were obtained from a variety of public statistics, government reports, and technical literature sources. Supplementary Table 1 and 'Input Data' Excel file give the source for each input parameter and the dynamic input numbers for each oilfield, respectively. In some cases, data were digitized from literature plots[29], which may introduce minor inaccuracies due to pixel-based interpolation (these errors are likely to be small in comparison to other approximations such as model defaults). In cases where high temporal resolution (that is, monthly) data are reported, all data are converted to yearly averages.

References

25. Höök, M., Hirsch, R. & Aleklett, K. Giant oil field decline rates and their influence on world oil production. *Energy Policy* **37,** 2262–2272 (2009).
26. Tripathi, V. S. & Brandt, A. R. Estimating decades-long trends in petroleum field energy return on investment (EROI) with an engineering-based model. *PLoS ONE* **12,** e0171083 (2017).
27. El-Houjeiri, H. M., Brandt, A. R. & Duffy, J. E. Open-source LCA tool for estimating greenhouse gas emissions from crude oil production using field characteristics. *Environ. Sci. Technol.* **47,** 5998–6006 (2013).
28. Brandt, A. R. Embodied energy and GHG emissions from material use in conventional and unconventional oil and gas operations. *Environ. Sci. Technol.* **49,** 13059–13066 (2015).
29. Rohatgi, A. WebPlotDigitizer v.3.9 (October 2015, accessed February 2017); http://arohatgi.info/WebPlotDigitizer